Planck 2013 constraints on inflation

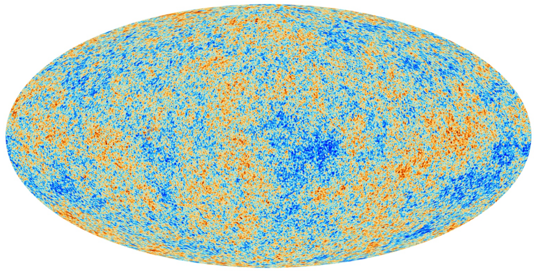

Fabio Finelli

INAF/IASF Bologna

INFN - Sezione di Bologna

On behalf of the Planck Collaboration

Planck 2013 Results XXII: Constraints on Inflation

Santander, June 24th, 2013

Exploring the Physics of Inflation

Outline

- Introduction: essential for inflation
- Likelihood Inputs for Planck analysis
- Planck 2013 constraints on single field inflation
- Planck 2013 constraints on initial conditions and implications for multi-field inflation

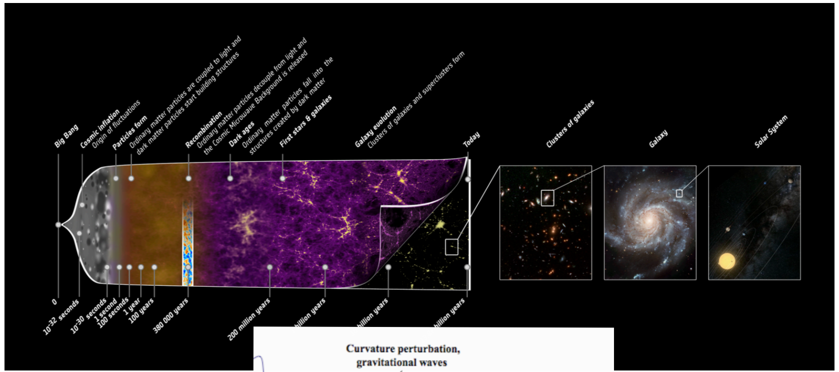
Big Bang
Cosmic inflation
Origin of fluctuations
Particles form
Ordinary matter particles are coupled to light and dark matter particles start building structures
Recombination
Ordinary matter particles decouple from light and the Cosmic Microwave Background is released
Dark ages
Ordinary matter particles fall into the structures created by dark matter
First stars & galaxies
Galaxy evolution
Clusters of galaxies and superclusters form
Today
Clusters of galaxies
Galaxy
Solar System
0
10^{-32} seconds
10^{-30} seconds
1 second
100 seconds
1 year
100 years
380 000 years
200 million years

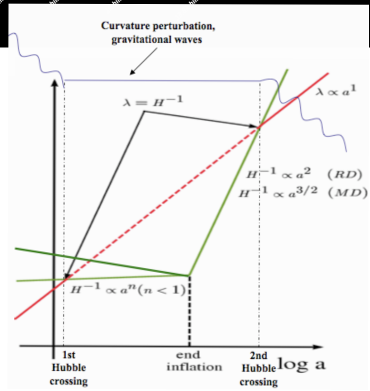
Curvature perturbation,
gravitational waves
$\lambda = H^{-1}$
$\lambda \propto a^1$
$H^{-1} \propto a^2 \quad (RD)$
$H^{-1} \propto a^{3/2} \quad (MD)$
$H^{-1} \propto a^n (n < 1)$
1st Hubble crossing
end inflation
2nd Hubble crossing
log a

Generation of fluctuations

The quantum fluctuations associated to scalar and tensor modes are amplified by the nearly exponential expansion to squeezed states on super-Hubble scales (which resemble classical states).

Slow-roll of the classical inflaton on a smooth potential

$$3H\dot{\phi} \approx -V_\phi$$

$$H^2 \approx \frac{V}{3{M_{\rm pl}}^2}$$

$$g_{\mu\nu}(t) + \delta g_{\mu\nu}(t, \vec{x})$$

Gravitational Waves h^{TT}

$$(ah_k^{+,\times})'' + \left(k^2 - \frac{a''}{a}\right)(ah_k^{+,\times}) = 0$$

Grischuck 1972

Starobinsky 1979

Rubakov et al 1982

Fabbri & Pollock 1983

Abbott & Wise 1984

$$\phi(t) + \phi(t, \vec{x})$$

Scalar Perturbations Q (Q is the g.i fluctuation associated to the Klein-Gordon inflaton)

$$(a\delta\phi_k)'' + \left(k^2 - \frac{z''}{z}\right)(a\delta\phi_k) = 0$$

$$z = a\dot{\phi}/H$$

Mukhanov 1985, 1988

Sasaki 1986

Slow-roll predictions

$$\mathcal{P}_{\rm t}(k) = \frac{4k^3}{\pi^2}\frac{|h_k|^2}{M_{\rm pl}^2} = A_{\rm t}\left(\frac{k}{k_*}\right)^{n_{\rm t}+\frac{1}{2}\,{\rm d}n_{\rm t}/{\rm d}\ln k\,\ln(k/k_*)+\ldots}$$

$$\mathcal{P}_{\mathcal{R}}(k) = \frac{k^3}{2\pi^2}\frac{H^2|Q_k|^2}{\dot\phi^2} = A_{\rm s}\left(\frac{k}{k_*}\right)^{n_{\rm s}-1+\frac{1}{2}\,{\rm d}n_{\rm s}/{\rm d}\ln k\,\ln(k/k_*)+\frac{1}{6}\,{\rm d}^2n_{\rm s}/{\rm d}\ln k^2(\ln(k/k_*))^2+\ldots}$$

Amplitude and tilts of curvature and tensor perturbation are linked to the physics of inflation to first order in slow-roll parameters

$$\epsilon_V = \frac{M_{\rm pl}^2 V_\phi^2}{2V^2} \qquad \eta_V = \frac{M_{\rm pl}^2 V_{\phi\phi}}{V} \qquad \xi_V^2 = \frac{M_{\rm pl}^4 V_\phi V_{\phi\phi\phi}}{V^2} \qquad \varpi_V^3 = \frac{M_{\rm pl}^6 V_\phi^2 V_{\phi\phi\phi\phi}}{V^3}$$

To lowest order in slow-roll parameters:

$$\begin{aligned}
A_{\rm s} &\approx \frac{V}{24\pi^2 M_{\rm pl}^4 \epsilon_V}\\
A_{\rm t} &\approx \frac{2V}{3\pi^2 M_{\rm pl}^4}\\
n_{\rm s}-1 &\approx 2\eta_V - 6\epsilon_V\\
n_{\rm t} &\approx -2\epsilon_V\\
{\rm d}n_{\rm s}/{\rm d}\ln k &\approx +16\epsilon_V\eta_V - 24\epsilon_V^2 - 2\xi_V^2\\
{\rm d}n_{\rm t}/{\rm d}\ln k &\approx +4\epsilon_V\eta_V - 8\epsilon_V^2\\
{\rm d}^2n_{\rm s}/{\rm d}\ln k^2 &\approx -192\epsilon_V^3 + 192\epsilon_V^2\eta_V - 32\epsilon_V\eta_V^2\\
&\quad - 24\epsilon_V\xi_V^2 + 2\eta_V\xi_V^2 + 2\varpi_V^3
\end{aligned}$$

under the assumption of a standard kinetic term (Klein-Gordon Lagrangian), Bunch-Davies vacuum, featureless potential.

Slow-roll predictions: 2

Tensor spectral index fixed to the tensor-to-scalar ratio by the so-called consistency condition for a standard kinetic term:

$$r = \frac{\mathcal{P}_{\rm t}(k_*)}{\mathcal{P}_{\mathcal{R}}(k_*)} \approx 16\epsilon_V \approx -8n_{\rm t}$$

For a standard kinetic term:

$f_{\rm NL} \approx \mathcal{O}(\epsilon_V\,, \eta_V)$ in agreement with the Planck constraints on the bispectrum.

Planck 2013 results XXIV:

Constraints on primordial non-Gaussianities

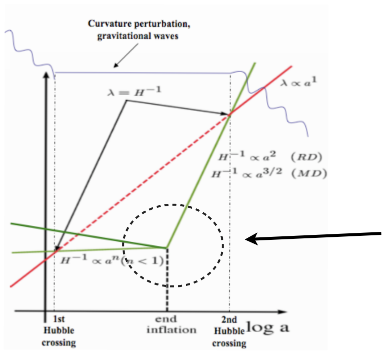

The main uncertainty arises in establishing the correspondence between the comoving wavenumber today, and the inflaton energy density when the mode of that wavenumber crossed the Hubble radius during inflation. This correspondence depends both on the inflationary model and on the cosmological evolution from the end of inflation to the present.

The slowly evolving potential and slow-roll parameters are evaluated when the wavelength crosses the Hubble radius N* e-folds before the end of inflation:

$$N_* = \int_{t_*}^{t_e} \mathrm{d}t\, H \approx \frac{1}{M_{\rm pl}^2} \int_{\phi_*}^{\phi_e} \mathrm{d}\phi\, \frac{V}{V_\phi}$$

$$N_* \approx 71.21 - \ln\left(\frac{k_*}{a_0 H_0}\right) + \frac{1}{4}\ln\left(\frac{V_{\rm hor}}{{\rm M_{pl}}^4}\right) + \frac{1-3w_{\rm int}}{12(1+w_{\rm int})}\ln\left(\frac{\rho_{\rm rh}}{\rho_{\rm end}}\right)$$

Standard choice to consider 50 < N < 60.

Cosmological Models

Given a model M with free n parameters ***x*** ≡ {$x_1, \cdots, x_n$} and a likelihood function of the data L(data|***x***), the (posterior) probability density P as a function of the parameters can be expressed as

$$\mathcal{P}(\hat{x}|\text{data}, \mathcal{M}) \propto \mathcal{L}(\text{data}|\hat{x}) \cdot P(\hat{x}|\mathcal{M})$$

where $P(\hat{x}|\mathcal{M})$ represents the data-independent prior probability density.

Parameter	Prior range	Baseline	Definition
$\omega_b \equiv \Omega_b h^2$	[0.005, 0.1]	...	Baryon density today
$\omega_c \equiv \Omega_c h^2$	[0.001, 0.99]	...	Cold dark matter density today
$100\theta_{MC}$	[0.5, 10.0]	...	100 × approximation to r_*/D_A (CosmoMC)
τ	[0.01, 0.8]	...	Thomson scattering optical depth due to reionization
Ω_K	[−0.3, 0.3]	0	Curvature parameter today with $\Omega_{tot} = 1 - \Omega_K$
$\sum m_\nu$	[0, 5]	0.06	The sum of neutrino masses in eV
$m^{eff}_{\nu,\,sterile}$	[0, 3]	0	Effective mass of sterile neutrino in eV
w_0	[−3.0, −0.3]	−1	Dark energy equation of state[a], $w(a) = w_0 + (1-a)w_a$
w_a	[−2, 2]	0	As above (perturbations modelled using PPF)
N_{eff}	[0.05, 10.0]	3.046	Effective number of neutrino-like relativistic degrees of freedom (see text)
Y_P	[0.1, 0.5]	BBN	Fraction of baryonic mass in helium
A_L	[0, 10]	1	Amplitude of the lensing power relative to the physical value
n_s	[0.9, 1.1]	...	Scalar spectrum power-law index ($k_0 = 0.05\,\mathrm{Mpc}^{-1}$)
n_t	$n_t = -r_{0.05}/8$	Inflation	Tensor spectrum power-law index ($k_0 = 0.05\,\mathrm{Mpc}^{-1}$)
$dn_s/d\ln k$	[−1, 1]	0	Running of the spectral index
$\ln(10^{10}A_s)$	[2.7, 4.0]	...	Log power of the primordial curvature perturbations ($k_0 = 0.05\,\mathrm{Mpc}^{-1}$)
$r_{0.05}$	[0, 2]	0	Ratio of tensor primordial power to curvature power at $k_0 = 0.05\,\mathrm{Mpc}^{-1}$

planck

Likelihood inputs: Planck TT

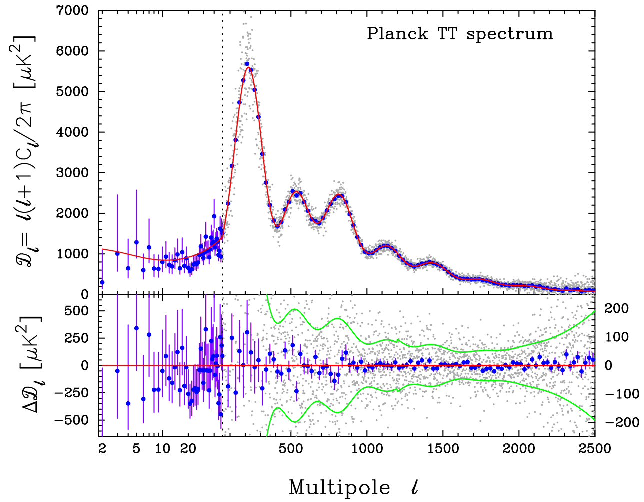

The Planck CMB likelihood is based on a hybrid approach:

a. Gaussian likelihood approximation based on temperature pseudo cross-spectra

b. Map based temperature and polarization likelihood at low multipoles.

The small-scale Planck temperature likelihood is based on pseudo cross-spectra between pairs of maps at

100 GHz $f_{sky} = 0.49$ $50 < \ell < 1200$
143 GHz $f_{sky} = 0.31$ $50 < \ell < 2000$
217 GHz $f_{sky} = 0.31$ $50 < \ell < 2500$ (for 143x217 as well)

The foreground model used in the Planck high-likelihood includes contributions to the auto and cross-frequency power spectra from unresolved radio point sources, CIB, tSZ and kSZ effects, for a total of **eleven** adjustable nuisance parameters. In the analysis **two** calibration parameters (for the 100 GHz and 217 GHz relative to the 143 GHz) and **one** amplitude for the dominant beam uncertainty are also left free to vary (the other beam uncertainties are marginalized analytically). The total sums to **fourteen** parameters for the high-ℓ likelihood.

Parameter	Prior range	Definition
A^{PS}_{100}	$[0, 360]$	Contribution of Poisson point-source power to $\mathcal{D}^{100\times100}_{3000}$ for *Planck* (in μK^2)
A^{PS}_{143}	$[0, 270]$	As for A^{PS}_{100}, but at 143 GHz
A^{PS}_{217}	$[0, 450]$	As for A^{PS}_{100}, but at 217 GHz
$r^{PS}_{143\times217}$	$[0, 1]$	Point-source correlation coefficient for *Planck* between 143 and 217 GHz
A^{CIB}_{143}	$[0, 20]$	Contribution of CIB power to $\mathcal{D}^{143\times143}_{3000}$ at the *Planck* CMB frequency for 143 GHz (in μK^2)
A^{CIB}_{217}	$[0, 80]$	As for A^{CIB}_{143}, but for 217 GHz
$r^{CIB}_{143\times217}$	$[0, 1]$	CIB correlation coefficient between 143 and 217 GHz
γ^{CIB}	$[-2, 2]$ (0.7 ± 0.2)	Spectral index of the CIB angular power ($\mathcal{D}_\ell \propto \ell^{\gamma^{CIB}}$)
A^{tSZ}	$[0, 10]$	Contribution of tSZ to $\mathcal{D}^{143\times143}_{3000}$ at 143 GHz (in μK^2)
A^{kSZ}	$[0, 10]$	Contribution of kSZ to $\mathcal{D}_{3000}$ (in μK^2)
$\xi^{tSZ\times CIB}$	$[0, 1]$	Correlation coefficient between the CIB and tSZ (see text)
c_{100}	$[0.98, 1.02]$ (1.0006 ± 0.0004)	Relative power spectrum calibration for *Planck* between 100 GHz and 143 GHz
c_{217}	$[0.95, 1.05]$ (0.9966 ± 0.0015)	Relative power spectrum calibration for *Planck* between 217 GHz and 143 GHz
β^i_j	(0 ± 1)	Amplitude of the jth beam eigenmode ($j = 1$–5) for the ith cross-spectrum ($i = 1$–4)

The low-ℓ Planck likelihood combines the Planck temperature data with the large angular scale 9-year WMAP polarization data for this release. Following Page et al. 2006, the temperature and polarization likelihood can be separated assuming negligible noise in the temperature map.

The temperature likelihood is based on a Gibbs approach, mapping out the distribution of the $\ell < 50$ CMB multipoles from a foreground-cleaned combination of the 30-353 GHz maps.

The polarization likelihood uses a pixel-based approach using the WMAP 9-year polarization maps at 33, 41, and 61GHz , and includes the temperature-polarization cross-correlation. Its angular range is $\ell < 23$ for TE, EE, and BB.

Planck 2013 results XXV: CMB power spectra and likelihood

Planck 2013 results XXVI: Cosmological parameters

Planck lensing

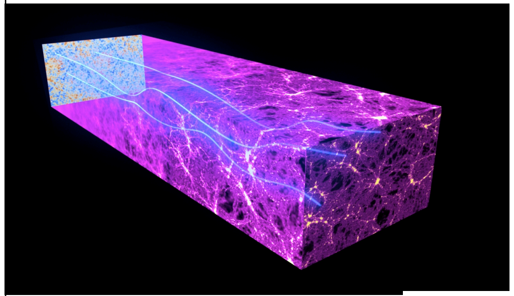

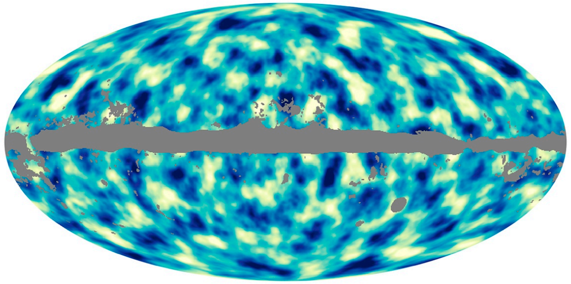

Credit: ESA and the Planck Collaboration.

planck

Santander, June 24th, 2013
Exploring the Physics of Inflation

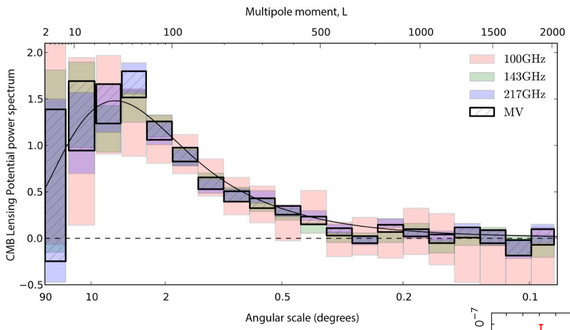

A detection of lensing > 25 σ

Credit: ESA and the Planck Collaboration.

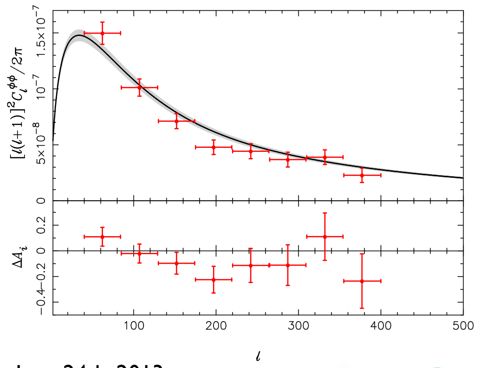

Planck 2013 results XVII: Gravitational lensing by large scale-structure

High-ℓ CMB

ACT (Atacama Cosmology Project) and SPT (South Pole Telescope).

ACT measures the power spectrum at 148 and 218 GHz, and the cross-spectrum, and covers angular scales 500 < ℓ < 10000 at 148 GHz and 1500 < ℓ < 10000 at 218 GHz. The range ℓ >1000 is used in combination with Planck.

SPT measures the power spectrum for angular scales 2000 < ℓ < 10000 at 95, 150, and 220 GHz

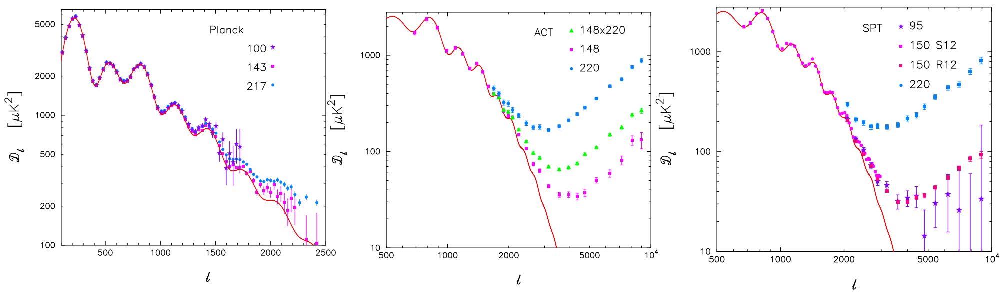

$A^{\mathrm{PS,\,ACT}}_{148}$	[0, 30]	Contribution of Poisson point-source power to $\mathcal{D}^{148\times148}_{3000}$ for ACT (in μK^2)
$A^{\mathrm{PS,\,ACT}}_{218}$	[0, 200]	As for $A^{\mathrm{PS,\,ACT}}_{148}$, but at 218 GHz
$r^{\mathrm{PS}}_{150\times220}$	[0, 1]	Point-source correlation coefficient between 150 and 220 GHz (for ACT and SPT)
$A^{\mathrm{ACTe}}_{\mathrm{dust}}$	[0, 5] (0.8 ± 0.2)	Contribution from Galactic cirrus to $\mathcal{D}_{3000}$ at 150 GHz for ACTe (in μK^2)
$A^{\mathrm{ACTs}}_{\mathrm{dust}}$	[0, 5] (0.4 ± 0.2)	As $A^{\mathrm{ACTe}}_{\mathrm{dust}}$, but for ACTs
y^{ACTe}_{148}	[0.8, 1.3]	Map-level calibration of ACTe at 148 GHz relative to *Planck* 143 GHz
y^{ACTe}_{217}	[0.8, 1.3]	As y^{ACTe}_{148}, but at 217 GHz
y^{ACTs}_{148}	[0.8, 1.3]	Map-level calibration of ACTs at 148 GHz relative to *Planck* 143 GHz
y^{ACTs}_{217}	[0.8, 1.3]	As y^{ACTs}_{148}, but at 217 GHz
$A^{\mathrm{PS,\,SPT}}_{95}$	[0, 30]	Contribution of Poisson point-source power to $\mathcal{D}^{95\times95}_{3000}$ for SPT (in μK^2)
$A^{\mathrm{PS,\,SPT}}_{150}$	[0, 30]	As for $A^{\mathrm{PS,\,SPT}}_{95}$, but at 150 GHz
$A^{\mathrm{PS,\,SPT}}_{220}$	[0, 200]	As for $A^{\mathrm{PS,\,SPT}}_{95}$, but at 220 GHz
$r^{\mathrm{PS}}_{95\times150}$	[0, 1]	Point-source correlation coefficient between 95 and 150 GHz for SPT
$r^{\mathrm{PS}}_{95\times220}$	[0, 1]	As $r^{\mathrm{PS}}_{95\times150}$, but between 95 and 220 GHz
y^{SPT}_{95}	[0.8, 1.3]	Map-level calibration of SPT at 95 GHz relative to *Planck* 143 GHz
y^{SPT}_{150}	[0.8, 1.3]	As for y^{SPT}_{95}, but at 150 GHz
y^{SPT}_{220}	[0.8, 1.3]	As for y^{SPT}_{95}, but at 220 GHz

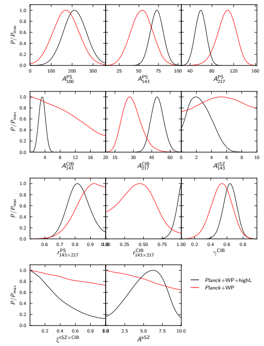

BAO

The Baryonic Acoustic Oscillation angular scale, extracted from galaxy redshift surveys, acts as a standard ruler and provides a constraint on the late-time geometry, breaking degeneracies with other cosmological parameters. These are the same oscillations we see on the CMB power spectrum, but now in the distribution of galaxies.

In this analysis we consider a combination of the measurements by the 6dFGRS (z= 0.106), SDSS-II (z = 0.35), and BOSS CMASS (z = 0.57) surveys, assuming no correlation between the three data points. We do not consider WiggleZ.

Fig. 15. Acoustic-scale distance ratio $r_s/D_V(z)$ divided by the distance ratio of the *Planck* base ΛCDM model. The points are colour-coded as follows: green star (6dF); purple squares (SDSS DR7 as analyzed by Percival et al. 2010); black star (SDSS DR7 as analyzed by Padmanabhan et al. 2012); blue cross (BOSS DR9); and blue circles (WiggleZ). The grey band shows the approximate ±1σ range allowed by *Planck* (computed from the CosmoMC chains).

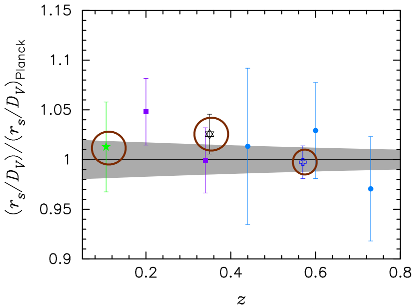

Baseline ΛCDM

	Planck		*Planck*+lensing		*Planck*+WP	
Parameter	Best fit	68% limits	Best fit	68% limits	Best fit	68% limits
$\Omega_b h^2$	0.022068	0.02207 ± 0.00033	0.022242	0.02217 ± 0.00033	0.022032	0.02205 ± 0.00028
$\Omega_c h^2$	0.12029	0.1196 ± 0.0031	0.11805	0.1186 ± 0.0031	0.12038	0.1199 ± 0.0027
$100\theta_{MC}$	1.04122	1.04132 ± 0.00068	1.04150	1.04141 ± 0.00067	1.04119	1.04131 ± 0.00063
τ	0.0925	0.097 ± 0.038	0.0949	0.089 ± 0.032	0.0925	$0.089^{+0.012}_{-0.014}$
n_s	0.9624	0.9616 ± 0.0094	0.9675	0.9635 ± 0.0094	0.9619	0.9603 ± 0.0073
$\ln(10^{10} A_s)$	3.098	3.103 ± 0.072	3.098	3.085 ± 0.057	3.0980	$3.089^{+0.024}_{-0.027}$

Planck 2013 results XXVI: Cosmological parameters

WMAP 9 yr result: $\tau = 0.089 \pm 0.014$

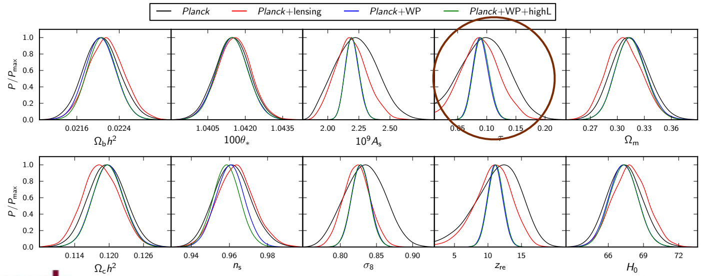

planck

Santander, June 24th, 2013
Exploring the Physics of Inflation

HZ

A scale invariant spectrum for curvature perturbations was proposed by Harrison, Zeldovich, Peebles and Yu as an explanation of observations at the begininning of 70's.

n_s=1 is a threshold value for blue scalar spectral index for inflationary models.

For scalar field driven inflation, n_s=1 can be obtained with $r \neq 0$.

	HZ	HZ + Y_P	HZ + N_{eff}	ΛCDM
$10^5\Omega_b h^2$	2296 ± 24	2296 ± 23	2285 ± 23	2205 ± 28
$10^4\Omega_c h^2$	1088 ± 13	1158 ± 20	1298 ± 43	1199 ± 27
$100\,\theta_{MC}$	1.04292 ± 0.00054	1.04439 ± 0.00063	1.04052 ± 0.00067	1.04131 ± 0.00063
τ	$0.125^{+0.016}_{-0.014}$	$0.109^{+0.013}_{-0.014}$	$0.105^{+0.014}_{-0.013}$	$0.089^{+0.012}_{-0.014}$
$\ln(10^{10}A_s)$	$3.133^{+0.032}_{-0.028}$	$3.137^{+0.027}_{-0.028}$	$3.143^{+0.027}_{-0.026}$	$3.089^{+0.024}_{-0.027}$
n_s	—	—	—	0.9603 ± 0.0073
N_{eff}	—	—	3.98 ± 0.19	—
Y_P	—	0.3194 ± 0.013	—	—
$-2\Delta\ln(\mathcal{L}_{max})$	27.9	2.2	2.8	0

Table 3. Constraints on cosmological parameters and best-fit $-2\Delta\ln(\mathcal{L})$ with respect to the standard ΛCDM model, using *Planck*+*WP* data, testing the significance of the deviation from the HZ model.

When adding BAO, HZ plus Y_P or N_{eff} provide $-2\,\Delta\,\ln(L_{max}) = 4.6$ or 8.
Even with general reionization instead of the optical depth the HZ provides $-2\,\Delta\,\ln(L_{max}) = 12.5$

$n_s<1$

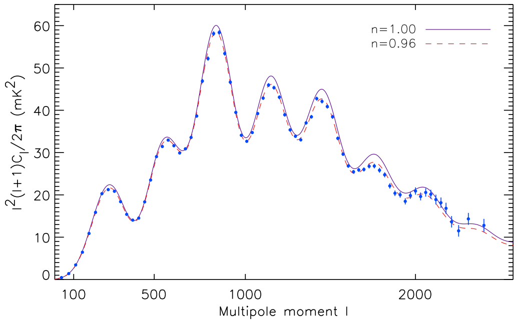

n_s = 0.9603±0.0073 *(68%; Planck*+WP)

n_s = 0.9585±0.0070 *(68%; Planck*+WP+highL)

n_s = 0.9608±0.0054 *(68%; Planck*+WP+BAO)

Planck 2013 results XXVI: Cosmological parameters

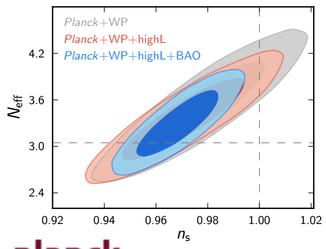

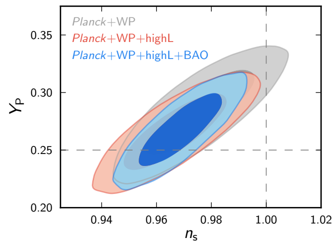

Tensors

$n_t \approx -r/8$

Model	Parameter	*Planck*+WP	*Planck*+WP+lensing	*Planck* + WP+high-ℓ	*Planck*+WP+BAO
ΛCDM + tensor	n_s	0.9624 ± 0.0075	0.9653 ± 0.0069	0.9600 ± 0.0071	0.9643 + 0.0059
	$r_{0.002}$	< 0.12	< 0.13	< 0.11	< 0.12
	$-2\Delta \ln \mathcal{L}_{max}$	0	0	0	-0.31

Table 4. Constraints on the primordial perturbation parameters in the ΛCDM+*r* model from *Planck* combined with other data sets. The constraints are given at the pivot scale $k_* = 0.002$ Mpc^{-1}.

The new bound from *Planck* is consistent with the limit from temperature anisotropies alone and improves on previous bounds: r <0.38 (WMAP 9), r<0.28 (WMAP 7+ACT 2013), r<0.18 (WMAP7 + SPT 12).

Current bounds based on B-polarization are weaker: r<0.73 (BICEP), r<2.8 (QUIET)

$$V_* < (1.94 \times 10^{16} \text{ GeV})^4 \quad \text{(95\%; } Planck\text{+WP)}$$

$$\frac{H_*}{M_{\rm pl}} < 3.7 \times 10^{-5} \quad \text{(95\%; } Planck\text{+WP)} \qquad M_{\rm pl} = 2.435 \times 10^{18} \text{GeV}$$

The precision in the determination of the higher acoustic peaks breaks the degeneracy n_s-r which has plagued previous experiments.

Planck vs the present...

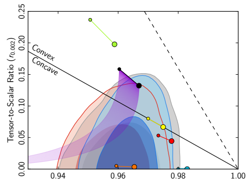

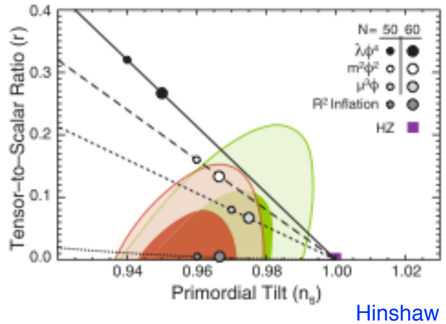

Green: eCMB

Red: eCMB + BAO + H_0

Hinshaw et al. 2012

... a brilliant future with Prism!

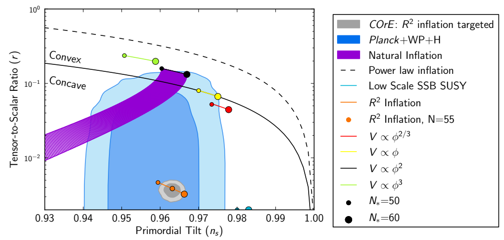

See Bucher's talk tomorrow

Inflationary Models

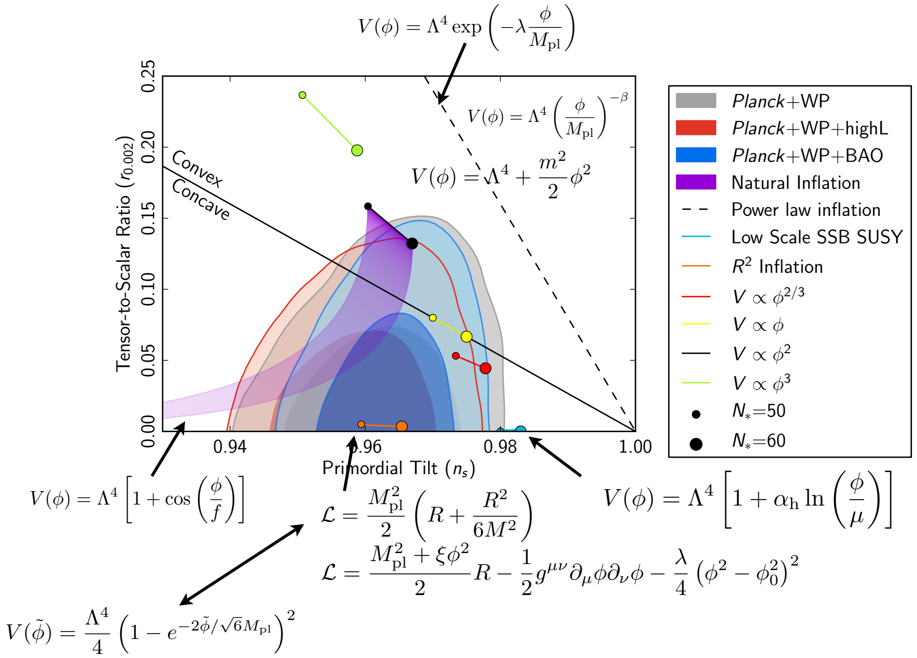

Robustness

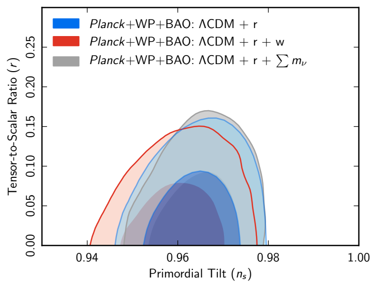

Planck+WP+BAO: ΛCDM + r
Planck+WP+BAO: ΛCDM + r + w
Planck+WP+BAO: ΛCDM + r + $\sum m_\nu$
Tensor-to-Scalar Ratio (r)
0.00 0.05 0.10 0.15 0.20 0.25
0.94 0.96 0.98 1.00
Primordial Tilt (n_s)

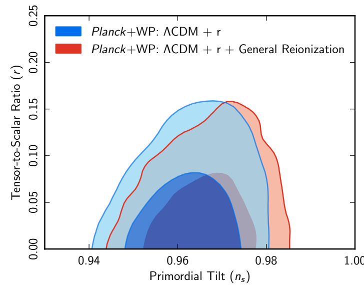

Planck+WP: ΛCDM + r
Planck+WP: ΛCDM + r + General Reionization
Tensor-to-Scalar Ratio (r)
0.00 0.05 0.10 0.15 0.20 0.25
0.94 0.96 0.98 1.00
Primordial Tilt (n_s)

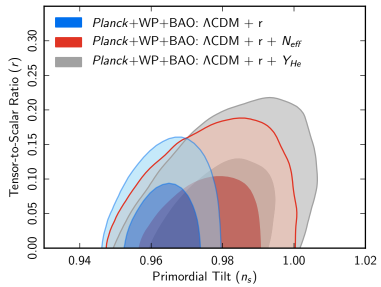

Planck+WP+BAO: ΛCDM + r
Planck+WP+BAO: ΛCDM + r + N_{eff}
Planck+WP+BAO: ΛCDM + r + Y_{He}
Tensor-to-Scalar Ratio (r)
0.00 0.05 0.10 0.15 0.20 0.25 0.30
0.94 0.96 0.98 1.00 1.02
Primordial Tilt (n_s)

Running

$$n_{s,t}(k) = n_{s,t}(k_*) + \frac{dn_{s,t}}{d\ln k}|_{k=k_*} \ln(k/k_*)$$

Kosowsky & Turner 1992

Generically non-zero, but small

Standard SR models predict O(10^{-3}), below *Planck* sensitivity

A hint for a negative running has been claimed in several previous investigations

WMAP 1 (Peiris et al. 2003): $dn_s/d\ln k = -0.055^{+0.028}_{-0.029}$ *(68%; WMAP 1 + 2dFGRS + Lyα)*

....

to SPT12 (Hou et al. 2013): $dn_s/d\ln k = -0.024 \pm 0.011$ *(68%; WMAP 7 + SPT 12)*

$dn_s/d\ln k = -0.028 \pm 0.010$ *(68%; WMAP 7 + SPT 12 + BAO + H_0)*

Such non-negligible running as from SPT12, roughly larger than one order of magnitude wtr to the predictions of the simplest SR models and of the same order of the tilts, would point to a very peculiar class of inflationary models in which the third derivative of the potential is not suppressed when the observable scales exit from the Hubble radius

$$\mathrm{d}n_s/\mathrm{d}\ln k \approx +16\epsilon_V\eta_V - 24\epsilon_V^2 - 2\xi_V^2$$

$$\xi_V^2 = \frac{M_{\rm pl}^4 V_\phi V_{\phi\phi\phi}}{V^2}$$

Such non-negligible running might also end inflation well before than 40-50 e-folds after the observable scales exit from the Hubble radius.

Model	Parameter	*Planck*+WP	*Planck*+WP+lensing	*Planck*+WP+high-ℓ	*Planck*+WP+BAO
ΛCDM + $dn_s/d\ln k$	n_s	0.9561 ± 0.0080	0.9615 ± 0.0072	0.9548 ± 0.0073	0.9596 ± 0.0063
	$dn_s/d\ln k$	-0.0134 ± 0.0090	-0.0094 ± 0.0085	-0.0149 ± 0.0085	-0.0130 ± 0.0090
	$-2\Delta \ln \mathcal{L}_{max}$	-1.50	-0.77	-2.95	-1.45
ΛCDM + $dn_s/d\ln k$ + $d^2n_s/d\ln k^2$	n_s	$0.9514^{+0.087}_{-0.090}$	$0.9573^{+0.077}_{-0.079}$	$0.9476^{+0.086}_{-0.088}$	$0.9568^{+0.068}_{-0.063}$
	$dn_s/d\ln k$	$0.001^{+0.016}_{-0.014}$	$0.006^{+0.015}_{-0.014}$	$0.001^{+0.013}_{-0.014}$	$0.000^{+0.016}_{-0.013}$
	$d^2n_s/d\ln k^2$	$0.020^{+0.016}_{-0.015}$	$0.019^{+0.018}_{-0.014}$	$0.022^{+0.016}_{-0.013}$	$0.017^{+0.016}_{-0.014}$
	$-2\Delta \ln \mathcal{L}_{max}$	-2.65	-2.14	-5.42	-2.40
ΛCDM + r + $dn_s/d\ln k$	n_s	0.9583 ± 0.0081	0.9633 ± 0.0072	0.9570 ± 0.0075	0.9607 ± 0.0063
	r	< 0.25	< 0.26	< 0.23	< 0.25
	$dn_s/d\ln k$	0.021 ± 0.012	0.017 ± 0.012	$-0.022^{+0.011}_{-0.010}$	$-0.021^{+0.012}_{+0.010}$
	$-2\Delta \ln \mathcal{L}_{max}$	-1.53	-0.26	-3.25	-1.5

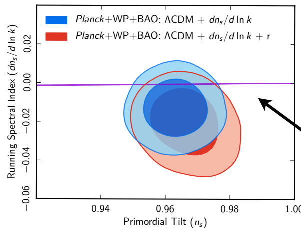

Chaotic monomial potential predictions

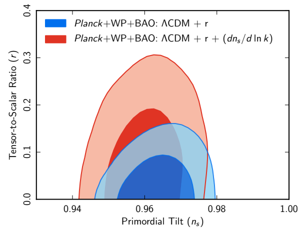

$$dn_s/d\ln k = -0.013 \pm 0.009$$

(68%; Planck+WP+BAO)

planck

Lack of power at low multipoles

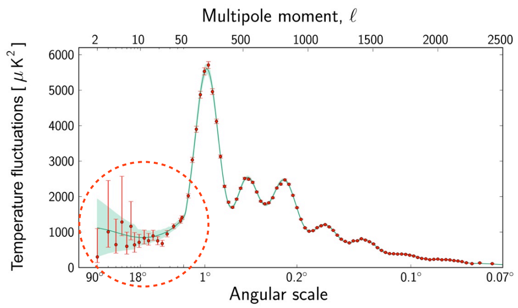

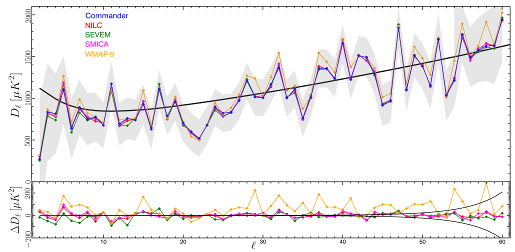

Ω_K

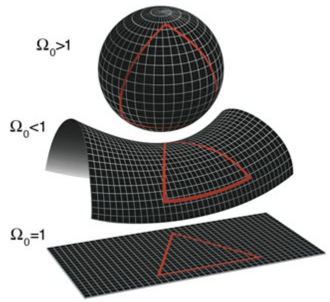

Credit: WMAP science team

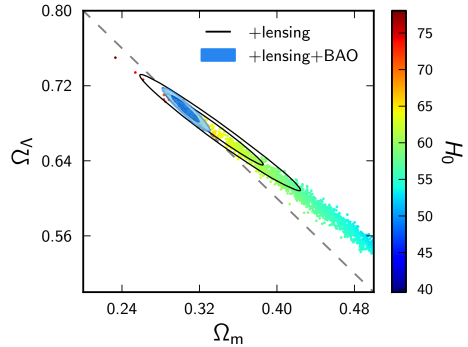

$\Omega_K = -0.042^{+0.043}_{-0.048}$ (95%; *Planck*+WP+highL)

$\Omega_K = -0.007^{+0.018}_{-0.020}$ (95%; *Planck*+lensing+WP)

$\Omega_K = -0.010^{+0.018}_{-0.019}$ (95%; *Planck*+lensing+WP+highL)

$\Omega_K = 0.000^{+0.0066}_{-0.0067}$ (95%; *Planck*+WP+BAO)

$\Omega_K = -0.0010^{+0.0062}_{-0.0065}$ (95%; *Planck*+lensing+WP+highL+BAO)

$\Omega_K + r$

$$\Omega_K = -0.0006 \pm 0.0069$$
$$r < 0.13$$

(95%; Planck+WP+BAO)

Including running (Ω_K + r + d n_s /d ln k):

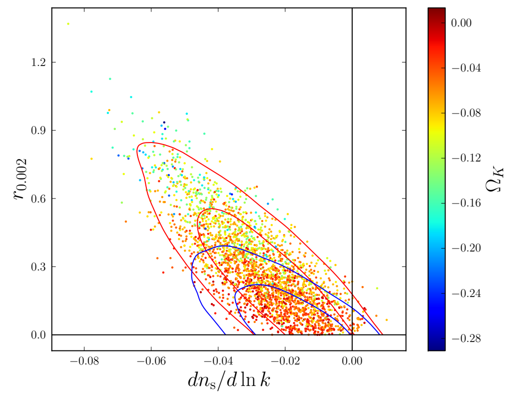

Constraints on post-inflationary epoch

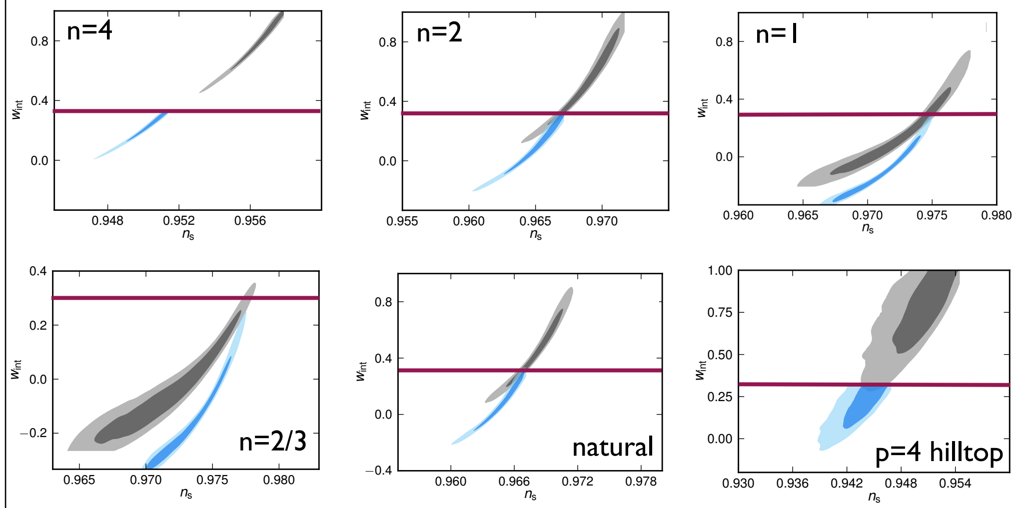

restrictive entropy generation

$$\rho_{\rm th}^{1/4} = 10^9 \quad w_{\rm int} \in [-1/3, 1/3]$$

permissive entropy generation

$$\rho_{\rm th}^{1/4} = 10^3 \quad w_{\rm int} \in [-1/3, 1]$$

Observable window of inflation

Relax the slow-roll approximation by evolving fluctuations numerically

Taylor expansion of the potential around the pivot scale up to fourth order

Conservative constraints since no assumption on how many e-folds before the end inflation these modes exit from the Hubble radius and the subsequent era are made.

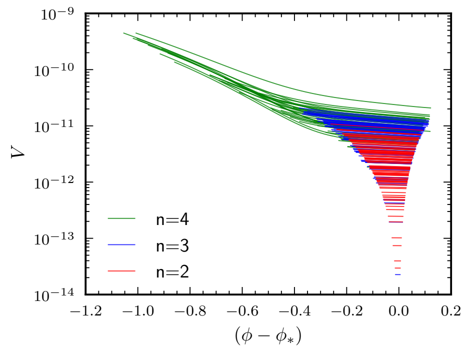

Lesgourgues & Valkenburg 2007

When the assumption of power-law spectra is relaxed, no “plateau” (ref. Ijjas, Steinhardt & Loeb, arXiv: 1304.2785) in the inflationary potential is seen (in qualitative analogy to the results obtained when the wavelength dependence of the spectral index is included). Planck points to a class of potentials, which might have interpretation for the subject of initial condition for the inflaton (ref. Hertog, arXiv: 1304.2785)

n	from $V(\phi)$ 2	3	4	from slow-roll
ϵ_V	< 0.0078	< 0.015	< 0.021	< 0.015
η_V	$-0.011^{+0.018}_{-0.015}$	$-0.016^{+0.028}_{-0.025}$	$0.022^{+0.052}_{-0.047}$	$-0.014^{+0.030}_{-0.022}$
ξ^2_V	–	$0.011^{+0.012}_{-0.011}$	$-0.015^{+0.031}_{-0.032}$	$0.009^{+0.011}_{-0.011}$
ϖ^3_V	–	–	$0.016^{+0.018}_{-0.019}$	–
$\Delta\chi^2_{\rm eff}$	0	-0.7	-3.7	-0.9

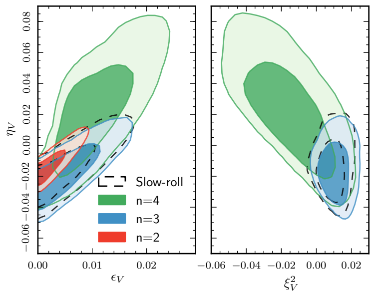

Planck + WP

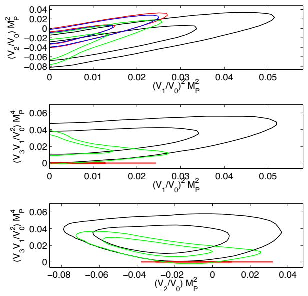

Finelli, Hamann, Leach, Lesgourgues, 2010
WMAP 5 plus SDSS DR 7

Planck measurement is probing slow-roll inflationary predictions essentially to second order.

Parametric searches for primordial power spectrum features

Mainly motivated by the anomalies at $\ell < 40$, various twists to the simplest SR inflationary models have been proposed.

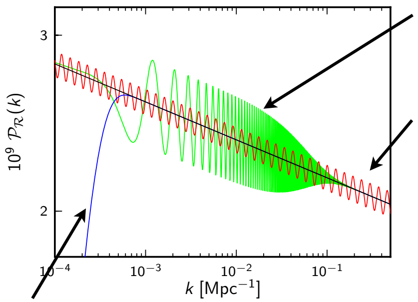

Feature in the potential:

$$V(\phi) = \frac{m^2}{2}\phi^2\left[1 + c\tanh\left(\frac{\phi - \phi_c}{d}\right)\right]$$

Non vacuum initial conditions/instanton effects in axion monodromy

$$V(\phi) = \mu^3\phi + \Lambda^4\cos\left(\frac{\phi}{f}\right)$$

$$\mathcal{P}_\mathcal{R}(k) = \mathcal{P}_0(k)\left\{1 + \alpha_\mathrm{w}\sin\left[\omega\ln\left(\frac{k}{k_*}\right) + \varphi\right]\right\}$$

Just enough e-folds, i.e. inflation as short as possible induce a cut-off in the primordial spectrum taken here as exponential

$$\mathcal{P}_\mathcal{R}(k) = \mathcal{P}_0(k)\left\{1 - \exp\left[-\left(\frac{k}{k_\mathrm{c}}\right)^{\lambda_\mathrm{c}}\right]\right\}$$

Model	$-2\Delta \ln \mathcal{L}_{max}$	$\ln B_{0X}$	Parameter	Best fit value
Wiggles	-9.0	1.5	α_w	0.0294
			ω	28.90
			φ	$0.075\ \pi$
Step-inflation	-11.7	0.3	$\mathcal{A}_f$	0.102
			$\ln(\eta_f/\mathrm{Mpc})$	8.214
			$\ln x_d$	4.47
Cutoff	-2.9	0.3	$\ln\left(k_c/\mathrm{Mpc}^{-1}\right)$	-8.493
			λ_c	0.474

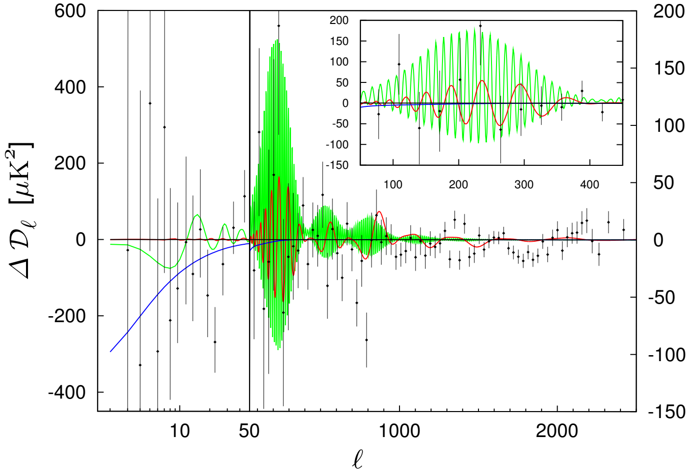

Reconstruction of the primordial power spectrum

Blind reconstruction of the primordial power spectrum from Planck data. *Bucher & Gauthier 2012*

Feature at ℓ = 1800, more prominently at 217 GHz. Origin probably not primordial.

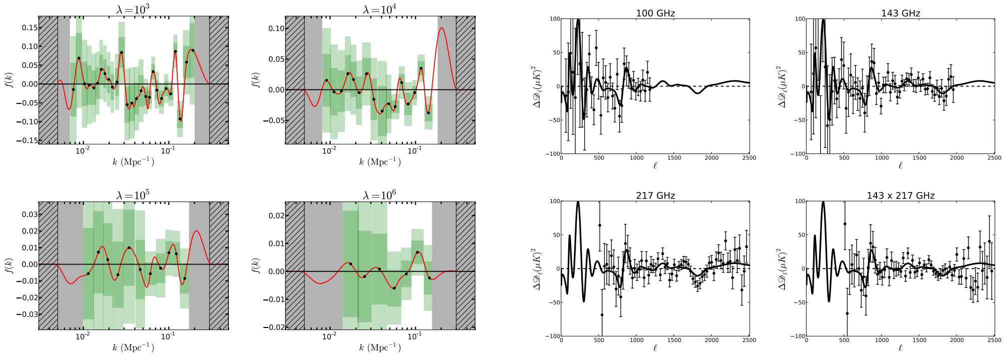

Combined analysis with f_{NL} constraints

Only through the combination of non-gaussianities constraints and temperature likelihood, non trivial constraints on inflation with generalized Lagrangian can be obtained.

$$c_s^2 = \frac{P_{,X}}{P_{,X} + 2XP_{,XX}}$$

$$\mathcal{L} = P(\phi, X)$$

$$X = -g^{\mu\nu}\partial_\mu\phi\partial_\nu\phi/2$$

$$r \simeq -8n_t c_s$$

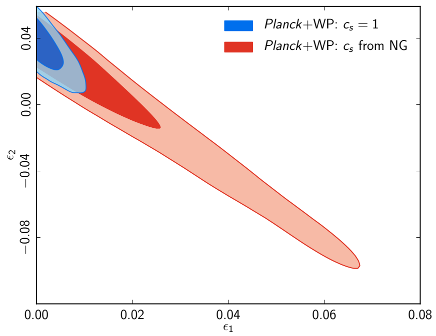

$c_s > 0.02$ (95%; *Planck*)

$\varepsilon_1 < 0.053$ (95%; *Planck*)

$c_s = 1$

$\varepsilon_1 < 0.008$ (95%; *Planck*)

DBI Model

$$P(\phi, X) = -f(\phi)^{-1}\sqrt{1 - 2f(\phi)X} + f(\phi)^{-1} - V(\phi)$$

$c_s > 0.07$ (95%; *Planck*)

$\varepsilon_1 < 0.042$ (95%; *Planck*)

Constraints on initial conditions

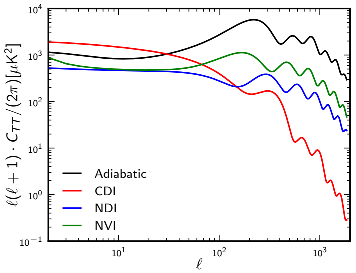

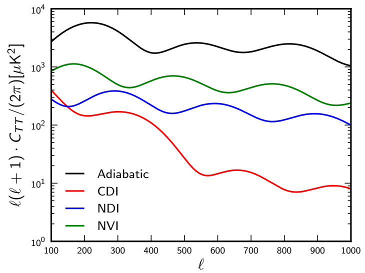

$$\mathcal{R} \approx C(k\tau)^\alpha \quad \text{for} \quad k\tau << 1$$

$\alpha = 0$ Curvature

$\alpha = 1$ $C \approx \Omega_c(\Omega_b)$ CDI(BI)

$\alpha = 1$ NVI

$\alpha = 2$ NDI

Bucher, Moodley, Turok, 2000

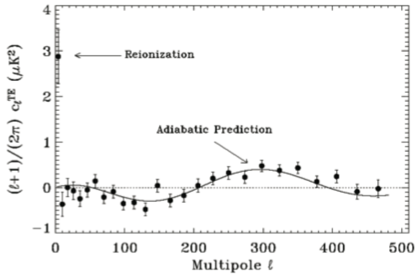

Hinshaw et al. 2003

Connection with multi-field inflation

Single field inflation cannot generate isocurvature fluctuations

Isocurvature perturbations can be generated in multi-field inflationary models:

$$\mathcal{R} = -H \frac{\sum_{i=1}^{N} \dot{\phi}_i Q_i}{\dot{\sigma}^2} \qquad \delta s_{ij} = \frac{\dot{\phi}_i Q_j - \dot{\phi}_j Q_i}{\dot{\sigma}}$$

$$\dot{\sigma}^2 \equiv \sum_{i=1}^{N} \dot{\phi}_i^2$$

Curvature and isocurvature fluctuations are generated with non-zero cross-correlation if the trajectory in the field space is curved.

Isocurvature fluctuations can feed curvature perturbation on large scales, but the opposite is not true

We study each isocurvature mode at a time.

Different parametrizations are available for the full general case including cross-correlation with non-trivial dependence on the wavelength.

We adopt a two-scale parametrization instead of an amplitude and a spectral tilt for the most general 6-parameter combination (k_1 =0.002 Mpc^{-1} and k_2 =0.1 Mpc^{-1}).
We also provide constraints at the standard *Planck* pivot scale k =0.05 Mpc^{-1}

$$\mathcal{P}_{\mathrm{ab}}(k) = \exp\left[\left(\frac{\ln(k)-\ln(k_2)}{\ln(k_1)-\ln(k_2)}\right)\ln(\mathcal{P}^{(1)}_{\mathrm{ab}}) + \left(\frac{\ln(k)-\ln(k_1)}{\ln(k_2)-\ln(k_1)}\right)\ln(\mathcal{P}^{(2)}_{\mathrm{ab}})\right]$$

$$\beta_{\mathrm{iso}}(k) = \frac{\mathcal{P}_{\mathcal{II}}(k)}{\mathcal{P}_{\mathcal{RR}}(k)+\mathcal{P}_{\mathcal{II}}(k)}$$

$$\alpha_{\mathcal{RR}}(\ell_{\mathrm{min}},\ell_{\mathrm{max}}) = \frac{(\Delta T)^2_{\mathcal{RR}}(\ell_{\mathrm{min}},\ell_{\mathrm{max}})}{(\Delta T)^2_{\mathrm{tot}}(\ell_{\mathrm{min}},\ell_{\mathrm{max}})}$$

$$\alpha_{\mathcal{RI}}(\ell_{\mathrm{min}},\ell_{\mathrm{max}}) = \frac{(\Delta T)^2_{\mathcal{RI}}(\ell_{\mathrm{min}},\ell_{\mathrm{max}})}{(\Delta T)^2_{\mathrm{tot}}(\ell_{\mathrm{min}},\ell_{\mathrm{max}})}$$

$$\alpha_{\mathcal{II}}(\ell_{\mathrm{min}},\ell_{\mathrm{max}}) = \frac{(\Delta T)^2_{\mathcal{II}}(\ell_{\mathrm{min}},\ell_{\mathrm{max}})}{(\Delta T)^2_{\mathrm{tot}}(\ell_{\mathrm{min}},\ell_{\mathrm{max}})}$$

$$(\Delta T)^2_X(\ell_{\mathrm{min}},\ell_{\mathrm{max}}) = \sum_{\ell=\ell_{\mathrm{min}}}^{\ell_{\mathrm{max}}}(2\ell+1)C^{TT}_{X,\ell}$$

Model	$\beta_{iso}(k_{low})$	$\beta_{iso}(k_{mid})$	$\beta_{iso}(k_{high})$	$\alpha_{\mathcal{RR}}^{(2,2500)}$	$\alpha_{\mathcal{II}}^{(2,2500)}$	$\alpha_{\mathcal{RI}}^{(2,2500)}$	Δn	$-2\Delta \ln \mathcal{L}_{max}$
Special CDM isocurvature cases:								
Uncorrelated, $n_{\mathcal{II}} = 1$, ("axion")	0.036	0.039	0.040	[0.98:1]	0.016	–	1	0
Fully correlated, $n_{\mathcal{II}} = n_{\mathcal{RR}}$, ("curvaton")	0.0025	0.0025	0.0025	[0.97:1]	0.0011	[0:0.028]	1	0
Fully anti-correlated, $n_{\mathcal{II}} = n_{\mathcal{RR}}$	0.0087	0.0087	0.0087	[1:1.06]	0.0046	[-0.067:0]	1	-1.3

Special cases for CDM isocurvature perturbations as:

- fully correlated, motivated by the curvaton scenario in which a second field, different from the inflaton, generates the primordial curvature perturbations by decaying into CDM.
- uncorrelated with a scale invariant spectrum, such as for an axion, a light and decoupled field during inflation.
- fully anti-correlated: as soon as we include an anti-correlation between curvature and CDM isocurvature a slight improvement in the $\Delta\chi^2$ emerges.

Fully correlated and uncorrelated perturbations are not preferred and strongly constrained, <0.0025 and <0.039 *(95%; Planck*+WP).

Implications for axion CDM isocurvature

The axion field was proposed to solve the strong CP problem and constitutes a well-motivated dark matter candidate. The axion is the Goldstone boson of the broken Peccei-Quinn (PQ) symmetry and may induce significant isocurvature perturbations: if inflation takes place after PQ symmetry breaking, the quantum fluctuations of the inflaton are responsible for primordial curvature perturbations, while those of the axion field generate primordial isocurvature perturbations.

After the QCD transition, when one of the vacua becomes preferred giving the axion field a mass, the axions behave as cold dark matter. This way of producing axionic dark matter is called the misalignment angle mechanism. In such a scenario, the CMB anisotropy may include significant power from CDM isocurvature fluctuations.

The case of uncorrelated adiabatic and scale-invariant isocurvature fluctuations has implications on the energy scale of inflation in this scenario:

$$H_{\rm inf} = \frac{0.96 \times 10^7 \ {\rm GeV}}{R_{\rm a}} \left(\frac{\beta_{\rm iso}}{0.04}\right)^{1/2} \left(\frac{\Omega_{\rm a}}{0.120}\right)^{1/2} \left(\frac{f_{\rm a}}{10^{11} \ {\rm GeV}}\right)^{0.408}$$

With the Planck constraint and under the assumption that CDM is fully constituted by axion:

$$H_{\rm inf} \leq 0.87 \times 10^7 \ {\rm GeV} \left(\frac{f_{\rm a}}{10^{11} \ {\rm GeV}}\right)^{0.408}$$

Implications for curvaton model

In the curvaton scenario primordial curvature perturbations are generated by a second field during inflation.

The Planck + WP constraints derived for fully correlated mixture of isocurvature and curvature perturbations have implications for the curvaton models under the hypothesis that CDM is created by the curvaton decay:

$$r_D = \frac{3\rho_{\rm curvaton}}{3\rho_{\rm curvaton} + 4\rho_{\rm radiation}} \qquad \beta_{\rm iso} = \frac{9(1-r_D)^2}{r_D^2 + 9(1-r_D)^2}$$

The constraint $r_D > 0.98$ (95%; Planck+WP) derived from isocurvature perturbations is consistent with the one derived from Planck non-gaussianities bound,

$$f_{\rm NL}^{\rm local} = \frac{5}{4r_D} - \frac{5}{3} - \frac{5r_D}{6} \qquad -1.25 < f_{\rm NL}^{\rm local} < -1.21 \qquad f_{\rm NL}^{\rm local} = 2.7 \pm 5.8$$

Planck 2013 results XXIV:

Constraints on primordial non-Gaussianities

General analysis

Model	$\beta_{iso}(k_{low})$	$\beta_{iso}(k_{mid})$	$\beta_{iso}(k_{high})$	$\alpha_{RR}^{(2,2500)}$	$\alpha_{II}^{(2,2500)}$	$\alpha_{RI}^{(2,2500)}$	Δn	$-2\Delta \ln \mathcal{L}_{max}$
General model:								
CDM isocurvature	0.075	0.39	0.60	[0.98:1.07]	0.039	[-0.093:0.014]	4	-4.6
ND isocurvature	0.27	0.27	0.32	[0.99:1.09]	0.093	[-0.18:0]	4	-4.2
NV isocurvature	0.18	0.14	0.17	[0.96:1.05]	0.068	[-0.090:0.026]	4	-2.5
Special CDM isocurvature cases:								
Uncorrelated, $n_{II} = 1$, ("axion")	0.036	0.039	0.040	[0.98:1]	0.016	–	1	0
Fully correlated, $n_{II} = n_{RR}$, ("curvaton")	0.0025	0.0025	0.0025	[0.97:1]	0.0011	[0:0.028]	1	0
Fully anti-correlated, $n_{II} = n_{RR}$	0.0087	0.0087	0.0087	[1:1.06]	0.0046	[-0.067:0]	1	-1.3

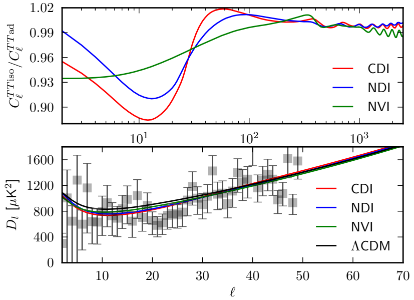

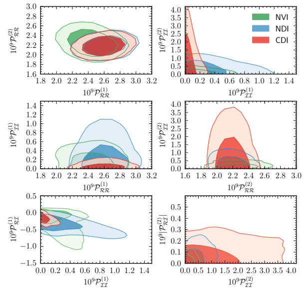

Conclusions

Standard single inflation is in agreement with the temperature and lensing power spectra of the Planck nominal mission. n_s =1 disfavoured at 6 sigma and r <0.11. Planck constraints on Ω_K and f_{NL} also support the prediction of the simplest models. Preference for a locally concave potential.

No statistical evidence of running spectral index (differently from WMAP 7 + SPT 12), Planck data cope with the slow-roll paradigm to second order.

First inflationary model proposed by Starobinsky in 1980 provide a good fit; same prediction of Higgs inflation.

Planck (+ WP) prefer adiabatic initial condition for primordial perturbations.

Large scale anomalies, such as low amplitude in the low multipoles, are not due to WMAP unaccounted systematics and are seen by *Planck* as well. Extensions of the minimal single field inflationary scenario can provide a theoretical framework for the anomalies at $\ell < 40$, as for the case of anti-correlated isocurvature perturbations, wavelength dependence of the scalar spectral index, cut-off of the primordial power spectrum, features in the inflationary potential.

Planck 2013 results

Planck 2013 results. I. Overview of products and scientific results
Planck 2013 results. II. The Low Frequency Instrument data processing
Planck 2013 results. III. LFI systematic uncertainties
Planck 2013 results. IV. Low Frequency Instrument beams and window functions
Planck 2013 results. V. LFI calibration
Planck 2013 results. VI. High Frequency Instrument data processing
Planck 2013 results. VII. HFI time response and beams
Planck 2013 results. VIII. HFI photometric calibration and mapmaking
Planck 2013 results. IX. HFI spectral responseremoval, and simulation
Planck 2013 results X. Energetic particle effects: characterization, removal, and simulation
Planck 2013 results. XII. Component separation
Planck 2013 results. XIII. Galactic CO emission
Planck 2013 results. XIV. Zodiacal emission
Planck 2013 results. XV. CMB power spectra and likelihood
Planck 2013 results. XVI. Cosmological parameters
Planck 2013 results. XVII. Gravitational lensing by large-scale structure
Planck 2013 results. XVIII. Gravitational lensing-infrared correlation
Planck 2013 results. XIX. The integrated Sachs-Wolfe effect
Planck 2013 results. XX. Cosmology from Sunyaev–Zeldovich cluster counts
Planck 2013 results. XXI. Cosmology with the all-sky Planck Compton parameter y-map
Planck 2013 results. XXII. Constraints on inflation
Planck 2013 results. XXIII. Isotropy and statistics of the CMB
Planck 2013 results. XXIV. Constraints on primordial non-Gaussianity
Planck 2013 results. XXV. Searches for cosmic strings and other topological defects
Planck 2013 results. XXVI. Background geometry and topology of the Universe
Planck 2013 results. XXVII. Doppler boosting of the CMB: Eppur si muove
Planck 2013 results. XXVIII. The Planck Catalogue of Compact Sources
Planck 2013 results. XXIX. Planck catalogue of Sunyaev–Zeldovich sources
Planck intermediate results. XIII. Constraints on peculiar velocities

HFF

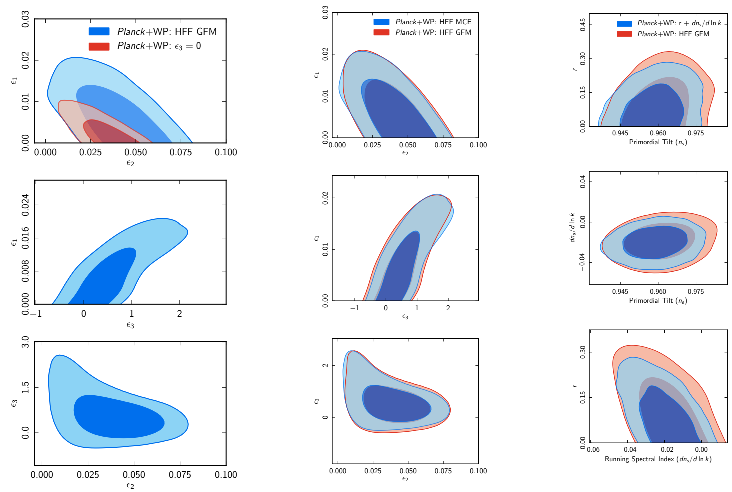

Planck+WP: HFF GFM
Planck+WP: $\epsilon_3 = 0$
Planck+WP: HFF MCE
Planck+WP: HFF GFM
Planck+WP: $r + dn_s/d\ln k$
Planck+WP: HFF GFM
ϵ_1
ϵ_2
ϵ_3
r
$dn_s/d\ln k$
Primordial Tilt (n_s)
Running Spectral Index ($dn_s/d\ln k$)